



Contents lists available at ScienceDirect

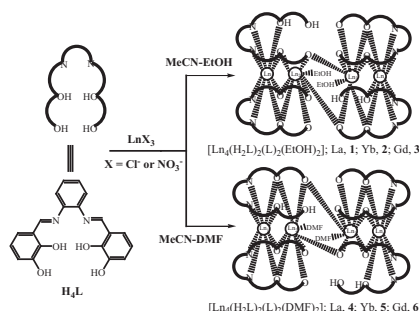
## Spectrochimica Acta Part A: Molecular and Biomolecular Spectroscopy

journal homepage: [www.elsevier.com/locate/saa](http://www.elsevier.com/locate/saa)Synthesis, characterization and oscillator-vibrated near-infrared (NIR) luminescence of two *pseudo*-polymorphic  $[\text{Yb}_4((\text{OH})_2\text{-Salophen})_4]$  complexesZhao Zhang<sup>a</sup>, Heini Feng<sup>a</sup>, Lin Liu<sup>a</sup>, Weixu Feng<sup>a</sup>, Chao Yu<sup>a</sup>, Xingqiang Lü<sup>a,\*</sup>, Wai-Kwok Wong<sup>b</sup>, Richard A. Jones<sup>c</sup><sup>a</sup>School of Chemical Engineering, Shaanxi Key Laboratory of Degradable Medical Material, Northwest University, Xi'an 710069, Shaanxi, China<sup>b</sup>Department of Chemistry, Hong Kong Baptist University, Waterloo Road, Kowloon Tong, Hong Kong, China<sup>c</sup>Department of Chemistry and Biochemistry, The University of Texas at Austin, 1 University Station A5300, Austin, TX 78712-0165, United States

## HIGHLIGHTS

- Dihydroxylated Salen-type ligand  $(\text{OH})_2\text{-Salophen}$ .
- *Pseudo*-polymorphic complexes  $[\text{Ln}_4((\text{OH})_2\text{-Salophen})_4]$ .
- Oscillator-vibrated NIR luminescence.

## GRAPHICAL ABSTRACT



## ARTICLE INFO

## Article history:

Received 19 August 2014

Received in revised form 14 January 2015

Accepted 29 January 2015

Available online 9 February 2015

## Keywords:

Tetranuclear  $[\text{Ln}_4((\text{OH})_2\text{-Salophen})_4]$ -arrayed complexes*Pseudo*-polymorphism

Oscillator-vibrated NIR luminescence

## ABSTRACT

Through the self-assembly of the  $(\text{OH})_2\text{-Salophen}$   $\text{H}_4\text{L}$  ( $\text{H}_4\text{L} = \text{N,N}'\text{-bis}(3\text{-hydroxylsalicylidene})\text{benzene-1,2-diamine}$ ) with  $\text{LnCl}_3 \cdot 6\text{H}_2\text{O}$  or  $\text{Ln}(\text{NO}_3)_3 \cdot 6\text{H}_2\text{O}$  ( $\text{Ln} = \text{La}, \text{Yb}$  or  $\text{Gd}$ ) in different solvent systems MeCN–EtOH and MeCN–DMF, the mixed  $(\text{L})^{4-}$  and  $(\text{H}_2\text{L})^{2-}$  coordination modes induce the formation of anion-independent while *pseudo*-polymorphic homoleptic linear tetranuclear complexes  $[\text{Ln}_4(\text{H}_2\text{L})_2(\text{L})_2(\text{EtOH})_2]$  ( $\text{Ln} = \text{La}, \mathbf{1}$ ;  $\text{Ln} = \text{Yb}, \mathbf{2}$  or  $\text{Ln} = \text{Gd}, \mathbf{3}$ ) and  $[\text{Ln}_4(\text{H}_2\text{L})_2(\text{L})_2(\text{DMF})_2]$  ( $\text{Ln} = \text{La}, \mathbf{4}$ ;  $\text{Ln} = \text{Yb}, \mathbf{5}$  or  $\text{Ln} = \text{Gd}, \mathbf{6}$ ), respectively. The result of their photophysical properties shows the characteristic NIR luminescence for both  $\text{Yb}^{3+}$ -based complexes  $\mathbf{2}$  and  $\mathbf{5}$  with emissive lifetimes in microsecond ranges, while the difference of nearby and/or distant oscillator-based ( $-\text{OH}$  and/or  $-\text{CH}$ ) vibrations from two coordinated EtOH or DMF molecules within the inner coordination spheres of  $\text{Yb}^{3+}$  ions in the two complexes has a decisive effect on their NIR luminescent properties.

© 2015 Elsevier B.V. All rights reserved.

## Introduction

Much recent interest has been devoted into near-infrared (NIR) luminescent polynuclear  $\text{Yb}^{3+}$  complexes with large Stokes' shift, long-lived lifetime ( $\mu\text{s}$  or  $\text{ms}$ ) and characteristic narrow-line

emission due to their potential applications in organic light-emitting diodes (OLEDs) [1], laser diodes [2] and fluoro-immunoassay [3]. However, on the one hand, the control on their molecular structures is synthetically challenging due to the variable coordination numbers and the flexible coordination geometries of  $\text{Yb}^{3+}$  ion [4], and the nature of counter-anions [5] and the reaction condition [6] also have the distinctive effects on the construction of the polynuclear  $\text{Yb}^{3+}$  complexes besides the character of the select-

\* Corresponding author. Tel./fax: +86 029 88302312.

E-mail addresses: [752201351@qq.com](mailto:752201351@qq.com), [lvxq@nwu.edu.cn](mailto:lvxq@nwu.edu.cn) (X. Lü).

ed organic ligands [7]. On the other hand, from the viewpoint of pursuit of enhanced NIR luminescent properties, the energy level's match between the excited states of the selected organic chromophore and  $\text{Yb}^{3+}$  ion [8] should be realized besides the complete avoiding or decreasing the luminescent quenching effect arising from OH-, CH- or NH-oscillators around the  $\text{Yb}^{3+}$  ions [9]. As a matter of fact, solvent-induced *pseudo*-polymorphism [10], as one common type of supramolecular isomerism, can give the similar polynuclear  $\text{Yb}^{3+}$  complexes from the same organic ligand, while different solvents are embracing the central  $\text{Yb}^{3+}$  ions. Therefore, the existence of different OH-, CH- or NH-containing solvents, especially within the inner coordination spheres of  $\text{Yb}^{3+}$  ions, endows a chance to study the detailed oscillator-vibrated NIR luminescence of the similar polynuclear  $\text{Yb}^{3+}$  complexes.

In contrast to the amounts of d and/or f-block complexes based on the typical Salen-type Schiff-base ligands [11], few examples on the complexes from the hydroxyl-modified Salen-type Schiff-base ligands are reported. In fact, the introduction of single or two hydroxyl groups on the Salen-type Schiff-base ligands endows the penta- or hexadentate coordination and the complicated charge balance modes in the construction of their complexes. For example, in our recent reports, discrete cyclic  $\text{Zn}_2\text{Ln}_2$  [12] or homoleptic  $\text{Ln}_6$ -arrayed complexes [13] have been obtained from the  $\text{N}_2\text{O}_3$ -quinquidentate (OH)-Salen Schiff-base ligands with the sole hydroxyl group on the corresponding linker, respectively, where the 3d  $\text{Zn}^{2+}$  Schiff-base complexes or the (OH)-Salen ligands could effectively sensitize the NIR luminescence of the central  $\text{Ln}^{3+}$  ions. As to the (OH)<sub>2</sub>-Salen ligands ( $\text{H}_4\text{L}^0$ ) with two hydroxyl groups at the *ortho* orientation to the phenoxide groups of Salen-type Schiff-base ligands, the possible multiple coordination modes (( $\text{L}^0$ )<sup>4-</sup>, ( $\text{HL}^0$ )<sup>3-</sup>, ( $\text{H}_2\text{L}^0$ )<sup>2-</sup> and ( $\text{H}_3\text{L}^0$ )<sup>-</sup>)-mode, as shown in Scheme 1S) should enrich their coordination chemistry. Till now, series of 3d  $\text{Zn}$ - [14], 5f  $\text{U}$ - [15], 3d  $\text{V}$ - and/or 5d  $\text{Re}$ - [16], and 3d(Cu/Ni)-5f(U) hetero-dinuclear complexes [17] were constructed from the ( $\text{L}^0$ )<sup>4-</sup> mode, while 5f  $\text{U}$ ,  $\text{U}_3$  or  $\text{U}_4$ -arrayed complexes [18] were obtained from the ( $\text{H}_2\text{L}^0$ )<sup>2-</sup>, ( $\text{L}^0$ )<sup>4-</sup> and ( $\text{HL}^0$ )<sup>3-</sup> or ( $\text{HL}^0$ )<sup>3-</sup> and ( $\text{H}_2\text{L}^0$ )<sup>2-</sup> modes of the (OH)<sub>2</sub>-Salen ligands, respectively. Nevertheless, to the best of our knowledge, no 4f  $\text{Ln}^{3+}$  complexes based on this kind of (OH)<sub>2</sub>-Salen ligands are reported, and the exploration on their photophysical properties is valuable. Herein, through the self-assembly from the (OH)<sub>2</sub>-Salophen ligand  $\text{H}_4\text{L}$  ( $\text{H}_4\text{L} = \text{N,N}'$ -bis(3-hydroxyl salicylidene)benzene-1,2-diamine) with  $\text{LnCl}_3 \cdot 6\text{H}_2\text{O}$  or  $\text{Ln}(\text{NO}_3)_3 \cdot 6\text{H}_2\text{O}$  ( $\text{Ln} = \text{La}$ ,  $\text{Yb}$  or  $\text{Gd}$ ) in different solvent systems, two series of anion-independent while *pseudo*-polymorphic [ $\text{Ln}_4(\text{H}_2\text{L})_2(\text{L})_2(\text{EtOH})_2$ ] ( $\text{Ln} = \text{La}$ , **1**;  $\text{Ln} = \text{Yb}$ , **2** or  $\text{Ln} = \text{Gd}$ , **3**) and [ $\text{Ln}_4(\text{H}_2\text{L})_2(\text{L})_2(\text{DMF})_2$ ] ( $\text{Ln} = \text{La}$ , **4**;  $\text{Ln} = \text{Yb}$ , **5** or  $\text{Ln} = \text{Gd}$ , **6**) with the similar homoleptic linear tetranuclear framework are obtained from the mixed coordination codes (( $\text{L}^0$ )<sup>4-</sup> and ( $\text{H}_2\text{L}^0$ )<sup>2-</sup> modes (in Scheme 2S) of four  $\text{HL}$  ligands, respectively. Moreover, based on the comparison of their photophysical properties, the NIR luminescence difference arisen from coordinated EtOH or DMF oscillators around the central  $\text{Yb}^{3+}$  ions is specially discussed.

## Experimental section

### Materials and methods

All chemicals were commercial products of reagent grade and were used without further purification. Elemental analyses were performed on a Perkin-Elmer 240C elemental analyzer. Infrared spectra were recorded on a Nicolet Magna-IR 550 spectrophotometer in the region 4000–400  $\text{cm}^{-1}$  using KBr pellets. <sup>1</sup>H NMR spectra were recorded on a JEOL EX270 spectrometer with  $\text{SiMe}_4$  as internal standard in  $\text{CDCl}_3$  or  $\text{DMSO}-d_6$  at room temperature. ESI-MS was performed on a Finnigan LCQ<sup>DECA</sup> XP HPLC-MS<sub>n</sub> mass

spectrometer with a mass to charge ( $m/z$ ) range of 4000 using a standard electrospray ion source and DMSO as solvent. Electronic absorption spectra in the UV/visible region were recorded with a Cary 300 UV spectrophotometer, and steady-state visible fluorescence, PL excitation spectra on a Photon Technology International (PTI) Alphascan spectrofluorometer and visible decay spectra on a pico-N<sub>2</sub> laser system (PTI Time Master). The quantum yield of the visible luminescence for each sample was determined by the relative comparison procedure, using a reference of a known quantum yield (quinine sulfate in dilute  $\text{H}_2\text{SO}_4$  solution,  $\Phi_{\text{em}} = 0.546$ ). NIR emission and excitation in solution were recorded by PTI QM4 spectrofluorometer with a PTI QM4 Near-Infrared InGaAs detector. The powder X-ray diffraction (PXRD) patterns were recorded on a D/Max-III A diffractometer with graphite-monochromatized  $\text{Cu K}\alpha$  radiation ( $\lambda = 1.5418 \text{ \AA}$ ). Thermogravimetric analyses (TGA) were carried out on a NETZSCH TG 209 instrument under flowing nitrogen by heating the samples from 40 to 600 °C.

### Synthesis

#### Synthesis of the (OH)<sub>2</sub>-Salophen ligand $\text{H}_4\text{L}$ ( $\text{H}_4\text{L} = \text{N,N}'$ -bis(3-hydroxylsalicylidene)benzene-1,2-diamine)

The (OH)<sub>2</sub>-Salophen ligand  $\text{H}_4\text{L}$  was prepared according to the procedure from the literature [19]. To a solution of *o*-phenylenediamine (1.08 g, 10 mmol) in absolute MeOH (10 ml), another solution of 2,3-dihydroxylbenzaldehyde (2.76 g, 20 mmol) in absolute MeOH (10 ml) was added, and the resulting mixture was refluxed under a  $\text{N}_2$  atmosphere for 3 h. After cooling to room temperature, the resultant red solution was left undisturbed a few days to evaporate in air, giving the red polycrystalline solid product in a yield of 61% (2.12 g). Calc. for  $\text{C}_{20}\text{H}_{16}\text{N}_2\text{O}_4$ : C, 68.96%; H, 4.63%; N, 8.04%; found: C, 68.92%; H, 4.71%; N, 8.01%. IR (KBr,  $\text{cm}^{-1}$ ): 3464 (b), 3055 (w), 2740 (w), 1618 (vs), 1579 (w), 1543 (w), 1521 (m), 1467 (s), 1415 (w), 1369 (s), 1280 (s), 1253 (s), 1209 (s), 1174 (m), 1103 (w), 1074 (m), 1051 (w), 1031 (w), 993 (w), 979 (w), 877 (m), 856 (s), 824 (w), 786 (m), 767 (w), 734 (w), 711 (m), 644 (m), 594 (s), 574 (s), 561 (s), 519 (m), 501 (m), 440 (m), 419 (w). <sup>1</sup>H NMR (400 MHz,  $\text{CDCl}_3$ ):  $\delta$  (ppm) 13.55 (s, 2H, —OH), 8.63 (s, 2H, —CH=N), 7.38 (t, 2H, —Ph), 7.28 (d, 2H, —Ph), 7.06 (d, 2H, —Ph), 6.98 (d, 2H, —Ph), 6.84 (d, 2H, —Ph), 5.93 (s, 2H, —OH).

#### Synthesis of complexes [ $\text{Ln}_4(\text{H}_2\text{L})_2(\text{L})_2(\text{EtOH})_2$ ] ( $\text{Ln} = \text{La}$ , **1**; $\text{Ln} = \text{Yb}$ , **2** or $\text{Ln} = \text{Gd}$ , **3**)

To a stirred solution of  $\text{H}_4\text{L}$  (0.10 mmol, 35.0 mg) and  $\text{Et}_3\text{N}$  (0.40 mmol, 50  $\mu\text{l}$ ) in absolute MeCN (8 ml), another solution of  $\text{LnCl}_3 \cdot 6\text{H}_2\text{O}$  (0.10 mmol,  $\text{Ln} = \text{La}$ , 35.3 mg;  $\text{Ln} = \text{Yb}$ , 38.8 mg;  $\text{Ln} = \text{Gd}$ , 37.2 mg) or  $\text{Ln}(\text{NO}_3)_3 \cdot 6\text{H}_2\text{O}$  (0.10 mmol,  $\text{Ln} = \text{La}$ , 43.3 mg;  $\text{Ln} = \text{Yb}$ , 46.7 mg or  $\text{Ln} = \text{Gd}$ , 45.1 mg) in absolute EtOH (8 ml) was added, and the mixture was refluxed under a  $\text{N}_2$  atmosphere for 3 h. After cooling to room temperature, the respective clear orange solution was filtered and diethyl ether was allowed to diffuse slowly into the filtrate at room temperature. Orange microcrystalline products of complexes **1–3** were obtained in about three weeks, respectively.

**For 1:** Yield: 20.8 mg, 41%. Calc. for  $\text{C}_{84}\text{H}_{64}\text{N}_8\text{O}_{18}\text{La}_4$ : C, 49.72%; H, 3.18%; N, 5.52%; found: C, 49.77%; H, 3.19%; N, 5.48%. IR (KBr,  $\text{cm}^{-1}$ ): 2931 (w), 2873 (w), 1652 (vs), 1614 (w), 1581 (w), 1558 (w), 1539 (m), 1506 (m), 1473 (m), 1460 (s), 1436 (w), 1419 (m), 1377 (s), 1336 (w), 1298 (w), 1274 (w), 1201 (s), 1190 (s), 1107 (w), 1082 (s), 972 (w), 873 (w), 866 (m), 833 (w), 785 (w), 732 (w), 675 (m), 648 (m), 567 (w), 472 (w), 457 (w). <sup>1</sup>H NMR (400 MHz,  $\text{DMSO}-d_6$ ):  $\delta$  (ppm) 9.45 (s, 2H, —OH), 8.61 (m, 4H, —CH=N), 8.51 (s, 4H, —CH=N), 7.97 (s, 8H, —Ph), 7.66 (m, 4H, —Ph), 7.39 (m, 4H, —Ph), 7.26 (m, 4H, —Ph), 7.08 (m, 2H, —Ph), 6.95 (m, 4H, —Ph), 6.68 (m, 2H, —Ph), 6.53 (m, 12H, —Ph), 6.29

(m, 2H, —OH), 2.69 (d, 2H, —OH), 2.34 (m, 4H, —CH<sub>2</sub>), 1.23 (m, 6H, —CH<sub>3</sub>). ESI-MS (DMSO) *m/z*: 2029.17432 (100%, [M—H]<sup>+</sup>).

For **2**: Yield: 23.8 mg, 44%. Calc. for C<sub>84</sub>H<sub>64</sub>N<sub>8</sub>O<sub>18</sub>Yb<sub>4</sub>: C, 46.59%; H, 2.98%; N, 5.17%; found: C, 46.41%; H, 2.78%; N, 5.14%. IR (KBr, cm<sup>-1</sup>): 2928 (w), 2871 (w), 1650 (vs), 1609 (w), 1580 (w), 1557 (w), 1538 (m), 1505 (m), 1472 (m), 1462 (s), 1431 (w), 1415 (m), 1373 (s), 1334 (w), 1297 (w), 1273 (w), 1201 (s), 1190 (s), 1109 (w), 1081 (s), 972 (w), 872 (w), 865 (m), 832 (w), 784 (w), 733 (w), 674 (m), 647 (m), 566 (w), 471 (w), 456 (w). ESI-MS (DMSO) *m/z*: 2188.44387 (100%, [M—Na]<sup>+</sup>).

For **3**: Yield: 24.7 mg, 47%. Calc. for C<sub>84</sub>H<sub>64</sub>N<sub>8</sub>O<sub>18</sub>Gd<sub>4</sub>: C, 47.99%; H, 3.07%; N, 5.33%; found: C, 47.81%; H, 3.06%; N, 5.28%. IR (KBr, cm<sup>-1</sup>): 2934 (w), 2875 (w), 1650 (vs), 1612 (w), 1581 (w), 1556 (w), 1537 (m), 1505 (m), 1472 (m), 1461 (s), 1435(w), 1419 (m), 1376 (s), 1332 (w), 1292 (w), 1278 (w), 1200 (s), 1193 (s), 1106 (w), 1085 (s), 971 (w), 872 (w), 865 (m), 832 (w), 785 (w), 730 (w), 673 (m), 644 (m), 566 (w), 471 (w), 453 (w). ESI-MS (DMSO) *m/z*: 2102.1134 (100%, [M—H]<sup>+</sup>).

#### Synthesis of complexes [Ln<sub>4</sub>(H<sub>2</sub>L)<sub>2</sub>(L)<sub>2</sub>(DMF)<sub>2</sub>] (Ln = La, **4**; Ln = Yb, **5** or Ln = Gd, **6**)

The synthesis of orange microcrystallines products of complexes **4–6** was in the same way as that of corresponding complexes **1–3** except that mixed solvents MeCN–DMF (v/v = 1/1) while not MeCN–EtOH (v/v = 1/1) were used.

For **4**: Yield: 18.8 mg, 36%. Calc. for C<sub>86</sub>H<sub>66</sub>N<sub>10</sub>O<sub>18</sub>La<sub>4</sub>: C, 49.59%; H, 3.19%; N, 6.72%; found: C, 49.47%; H, 3.25%; N, 6.68%. IR (KBr, cm<sup>-1</sup>): 2927 (w), 2887 (w), 1654 (vs), 1612 (w), 1602 (w), 1575 (w), 1541 (m), 1506 (m), 1487 (m), 1454 (s), 1398 (s), 1386 (s), 1328 (w), 1292 (w), 1251 (m), 1213 (w), 1190 (w), 1159 (m), 1107 (w), 1085 (w), 1045 (m), 1033 (w), 979 (w), 935 (w), 879 (w), 856 (w), 831 (m), 788 (s), 761 (w), 736 (w), 671 (w), 648 (w), 628 (w), 615 (w), 588 (w), 561 (w), 509 (w), 482 (w), 462 (w), 447 (w). <sup>1</sup>H NMR (400 MHz, DMSO-*d*<sub>6</sub>): δ (ppm) 9.46 (s, 2H, —OH), 8.62 (m, 4H, —CH=N), 8.50 (s, 4H, —CH=N), 8.01 (s, 8H, —Ph), 7.68 (m, 4H, —Ph), 7.43 (m, 4H, —Ph), 7.28 (m, 4H, —Ph), 7.13 (m, 2H, —Ph), 6.98 (m, 4H, —Ph), 6.71 (m, 2H, —Ph), 6.49 (m, 12 H, —Ph), 6.27 (m, 2H, —OH), 3.17 (s, 6H, —CH<sub>3</sub>), 3.08 (s, 6H, —CH<sub>3</sub>). ESI-MS (DMSO) *m/z*: 2105.69244 (100%, [M—Na]<sup>+</sup>).

For **5**: Yield: 21.6 mg, 39%. Calc. for C<sub>86</sub>H<sub>66</sub>N<sub>10</sub>O<sub>18</sub>Yb<sub>4</sub>: C, 46.54%; H, 3.00%; N, 6.31%; found: C, 46.47%; H, 3.08%; N, 6.24%. IR (KBr, cm<sup>-1</sup>): 2947 (w), 2898 (w), 1656 (vs), 1606 (w), 1581 (w), 1546 (m), 1514 (m), 1483 (m), 1460 (s), 1394 (s), 1331 (w), 1253 (m), 1193 (w), 1156 (m), 1103 (w), 1080 (w), 1051 (m), 1039 (w), 981 (w), 933 (w), 885 (w), 858 (w), 839 (m), 785 (s), 738 (w), 649 (w), 632 (w), 621 (w), 595 (w), 559 (w), 513 (w), 491 (w), 463 (w), 449 (w). ESI-MS (DMSO) *m/z*: 2242.36147 (100%, [M—Na]<sup>+</sup>).

For **6**: Yield: 23.2 mg, 43%. Calc. for C<sub>86</sub>H<sub>66</sub>N<sub>10</sub>O<sub>18</sub>Gd<sub>4</sub>: C, 47.90%; H, 3.08%; N, 6.50%; found: C, 47.81%; H, 3.16%; N, 6.48%. IR (KBr, cm<sup>-1</sup>): 2939 (w), 2896 (w), 1654 (vs), 1604(w), 1579 (w), 1543 (m), 1506 (m), 1485 (m), 1456 (s), 1398 (s), 1327 (w), 1287 (w), 1257 (m), 1210 (w), 1105 (w), 1083 (w), 1035 (m), 981 (w), 937 (m), 875 (w), 854 (w), 833 (w), 786 (w), 738 (w), 651 (w), 630 (w), 619 (w), 593 (w), 561 (w), 511 (w), 493 (w), 472 (w), 445 (w). ESI-MS (DMSO) *m/z*: 2179.44569 (100%, [M—Na]<sup>+</sup>).

#### Structure determination

Single crystals of complexes [Yb<sub>4</sub>(H<sub>2</sub>L)<sub>2</sub>(L)<sub>2</sub>(EtOH)<sub>2</sub>]-DMF (**2**-DMF) recrystallized from EtOH-DMF and [Yb<sub>4</sub>(H<sub>2</sub>L)<sub>2</sub>(L)<sub>2</sub>(DMF)<sub>2</sub>]-DMF·2MeOH·9H<sub>2</sub>O (**5**-DMF·2MeOH·9H<sub>2</sub>O) recrystallized from MeOH-DMF of suitable dimensions were mounted onto thin glass fibers. All the intensity data were collected on a Bruker SMART CCD diffractometer (Mo-Kα radiation and λ = 0.71073 Å) in ϕ and ω scan modes. Structures were solved by Direct methods followed by difference Fourier syntheses, and then refined by full-matrix

least-squares techniques against F<sup>2</sup> using SHELXTL [20]. All other non-hydrogen atoms were refined with anisotropic thermal parameters. Absorption corrections were applied using SADABS [21]. All hydrogen atoms were placed in calculated positions and refined isotropically using a riding model. Crystallographic data for complexes **2**-DMF and **5**-DMF·2MeOH·9H<sub>2</sub>O are presented in Table 1, and relevant atomic distances and bond angles are collected in Table S1, respectively.

## Results and discussion

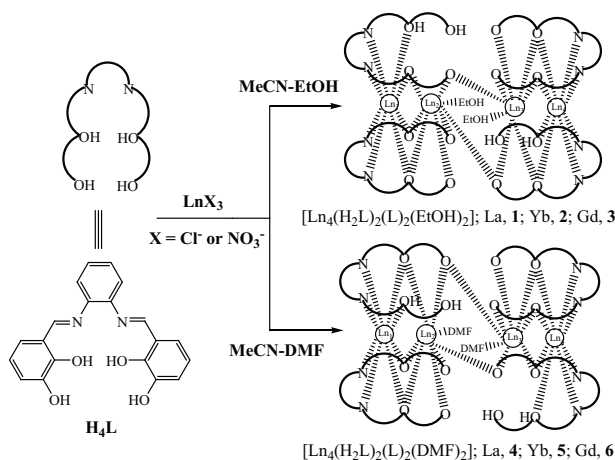
### Synthesis and characterization

As shown in Scheme 1, reaction of *o*-phenylenediamine with 2,3-dihydroxybenzaldehyde in 1:2 M ratio afforded the dihydroxylated (OH)<sub>2</sub>-Salophen ligand **H<sub>4</sub>L** in 61% yield. Further through the self-assembly of equimolar amounts of **H<sub>4</sub>L** with LnX<sub>3</sub>·6H<sub>2</sub>O (Ln = La, Yb, or Gd; X<sup>-</sup> = NO<sub>3</sub><sup>-</sup> or Cl<sup>-</sup>) in the presence of Et<sub>3</sub>N from the different mixed solvents (MeCN–EtOH or MeCN–DMF), two series of anion-independent while *pseudo*-polymorphic homoleptic tetranuclear complexes [Ln<sub>4</sub>(H<sub>2</sub>L)<sub>2</sub>(L)<sub>2</sub>(EtOH)<sub>2</sub>] (Ln = La, **1**; Ln = Yb, **2** or Ln = Gd, **3**) and [Ln<sub>4</sub>(H<sub>2</sub>L)<sub>2</sub>(L)<sub>2</sub>(DMF)<sub>2</sub>] (Ln = La, **4**; Ln = Yb, **5** or Ln = Gd, **6**) were obtained, respectively.

The (OH)<sub>2</sub>-Salophen ligand **H<sub>4</sub>L** and its two series of complexes **1–3** and **4–6** were well characterized by EA, FT-IR, <sup>1</sup>H NMR and ESI-MS. In the FT-IR spectra, the similar strong characteristic absorptions of the ν(C=N) vibration at 1650–1652 cm<sup>-1</sup> for **1–3** or 1654–1656 cm<sup>-1</sup> for complexes **4–6** are distinctively blue-shifted by 32–34 or 36–38 cm<sup>-1</sup> relative to that (1618 cm<sup>-1</sup>) of the free (OH)<sub>2</sub>-Salophen ligand **HL**, which should be attributed to the coordination of Ln<sup>3+</sup> ions. As to the room temperature <sup>1</sup>H NMR spectra (in Fig. 1S) of the two *anti*-ferromagnetic [La<sub>4</sub>((OH)<sub>2</sub>-Salophen)<sub>4</sub>]-arrayed complexes **1** and **4** in DMSO-*d*<sub>6</sub>, besides the disappearance of the typically intramolecular resonance-assisted hydrogen bonded (RAHB) O—H···N proton resonances (δ = 13.55 ppm) of the free **H<sub>4</sub>L** ligand, the resonances of the deprotonated ligands (δ = 9.45–1.23 ppm for **1** or δ = 9.46–3.08 ppm for **4**) are clearly more spread relative to those (δ = 8.63–5.93 ppm) of the free ligand **HL** up coordination of Ln<sup>3+</sup> ions. Moreover, the resonances of two kinds of down-field shifted free OH-based protons (δ = 9.45 and 6.29 ppm for **1** or δ = 9.46 and 6.27 ppm for **4**) are retained, showing the par-

**Table 1**  
Crystallographic data and structure refinement for **2**-DMF and **5**-DMF·2MeOH·9H<sub>2</sub>O.

Complexes	<b>2</b> -DMF	<b>5</b> -DMF·2MeOH·9H <sub>2</sub> O
Empirical formula	C <sub>87</sub> H <sub>71</sub> N <sub>9</sub> O <sub>19</sub> Yb <sub>4</sub>	C <sub>91</sub> H <sub>99</sub> N <sub>11</sub> O <sub>30</sub> Yb <sub>4</sub>
Formula weight	2238.69	2518.97
Crystal system	Monoclinic	Monoclinic
Space group	<i>P2(1)/c</i>	<i>P2(1)/c</i>
<i>a</i> (Å)	20.52(3)	20.264(6)
<i>b</i> (Å)	18.65(2)	18.236(5)
<i>c</i> (Å)	29.70(4)	29.037(8)
α (°)	90	90
β (°)	103.223(16)	104.050(4)
γ (°)	90	90
<i>V</i> (Å <sup>3</sup> )	11,066(24)	10,409(5)
<i>Z</i>	4	4
ρ (g cm <sup>-3</sup> )	1.344	1.607
Crystal size (mm)	0.31 × 0.28 × 0.25	0.34 × 0.30 × 0.26
μ (Mo-Kα) (mm <sup>-1</sup> )	3.407	3.639
Data/restraints/parameters	19,225/70/1072	23,836/27/1225
Quality-of-fit indicator	1.080	1.081
No. unique reflections	19,225	23,836
No. observed reflections	116,789	180,409
Final <i>R</i> indices [ <i>I</i> > 2σ( <i>I</i> )]	<i>R</i> <sub>1</sub> = 0.0710 <i>wR</i> <sub>2</sub> = 0.1880	<i>R</i> <sub>1</sub> = 0.0563 <i>wR</i> <sub>2</sub> = 0.1233
<i>R</i> indices (all data)	<i>R</i> <sub>1</sub> = 0.1050 <i>wR</i> <sub>2</sub> = 0.2041	<i>R</i> <sub>1</sub> = 0.1305 <i>wR</i> <sub>2</sub> = 0.1538



**Scheme 1.** Synthesis of the two series of solvent-induced *pseudo*-polymorphic complexes  $[\text{Ln}_4(\text{H}_2\text{L})_2(\text{L})_2(\text{EtOH})_2]$  ( $\text{Ln} = \text{La}$ , **1**;  $\text{Ln} = \text{Yb}$ , **2** or  $\text{Ln} = \text{Gd}$ , **3**) and  $[\text{Ln}_4(\text{H}_2\text{L})_2(\text{L})_2(\text{DMF})_2]$  ( $\text{Ln} = \text{La}$ , **4**;  $\text{Ln} = \text{Yb}$ , **5** or  $\text{Ln} = \text{Gd}$ , **6**).

tial deprotonations for two of four **HL** ligands in the formation of both **1** and **4**, and the new solvents-based proton resonances ( $\delta = 2.69\text{--}1.23$  ppm for the coordinated EtOH molecules in **1** or  $\delta = 3.17\text{--}3.08$  ppm for the coordinated DMF molecules in **4**) are observed in the up-field range, respectively. Especially, the ESI-MS spectra (Fig. 2S) of the two series of complexes **1–3** and complexes **4–6** in dilute DMSO display the similar patterns, where the strong mass peak at  $m/z$  2029.17432 (**1**), 2188.44387 (**2**), 2102.1134 (**3**), 2105.69244 (**4**), 2242.36147 (**5**) or 2179.44569 (**6**), assigned to the major species  $[\text{M}-\text{H}(\text{Na})]^+$  of complexes **1–6**, respectively. Both further indicate that each of the two series of discrete tetranuclear molecules **1–6** is retained in the respective dilute DMSO solution.

X-ray quality crystals of **2**:DMF as the representative of complexes **1–3** and **5**:DMF:2MeOH:9H<sub>2</sub>O as the representative of complexes **4–6** were obtained, and crystallographic data for the two complexes are presented in Tables 1 and 1S, respectively. Complex **2**:DMF crystallizes in the monoclinic space group  $P2(1)/c$ . For complex **2**:DMF, the structural unit is composed of one neutral  $[\text{Yb}_4(\text{H}_2\text{L})_2(\text{L})_2(\text{EtOH})_2]$  molecule and one solvate DMF. As shown in Fig. 1, two similar  $\text{Yb}_2(\text{L})(\text{H}_2\text{L})$  portions are bridged by two  $\mu\text{-O}$  phenoxide atoms (O8 and O13), in which O8 is from the deprotonated  $(\text{OH})_2\text{-Salophen}$  ligand ( $(\text{L})^{4-}$ -mode shown in Scheme 2S)

while O13 is from another partially deprotonated  $(\text{OH})_2\text{-Salophen}$  ligand ( $(\text{H}_2\text{L})^{2-}$ -mode shown in Scheme 2S), resulting in the formation of the homoleptic linear tetranuclear  $[\text{Yb}_4((\text{OH})_2\text{-Salophen})_4]$  host structure. In each of two similar  $\text{Yb}_2(\text{L})(\text{H}_2\text{L})$  moieties, although the two  $\text{Yb}^{3+}$  ions ( $\text{Yb1}$  and  $\text{Yb2}$ ) or ( $\text{Yb3}$  and  $\text{Yb4}$ ) are all eight-coordinate, one  $\text{Yb}$  ion ( $\text{Yb1}$  or  $\text{Yb4}$ ) is coupled into the two inner *cis*- $\text{N}_2\text{O}_2$  cores of two  $(\text{OH})_2\text{-Salophen}$  ligands, another  $\text{Yb}$  ion ( $\text{Yb2}$  or  $\text{Yb3}$ ) is linked by their corresponding two outer  $\text{O}_2\text{O}_2$  moieties. Each of the two unique inner  $\text{Yb}$  ions ( $\text{Yb1}$  or  $\text{Yb4}$ ) has the similar coordination environment, and is surrounded by two inner *cis*- $\text{N}_2\text{O}_2$  cores of two  $(\text{OH})_2\text{-Salophen}$  ligands with  $(\text{L})^{4-}$ -mode and  $(\text{H}_2\text{L})^{2-}$ -mode, respectively. As to the similar coordination environment outer  $\text{Yb}^{3+}$  ions ( $\text{Yb2}$  or  $\text{Yb3}$ ), in addition to six O atoms from two  $\text{O}_2\text{O}_2$  moieties of those two mixed-mode  $(\text{OH})_2\text{-Salophen}$  ligands, it saturates with O atom (O13 or O8) from the third  $(\text{H}_2\text{L})^{2-}$ -mode ligand of another  $\text{Yb}_2(\text{L})(\text{H}_2\text{L})$  portion and one O atom (O18 or O17) from the coordinated EtOH molecule. Three unique  $\text{Yb}\cdots\text{Yb}$  distances in the almost linear tetranuclear host structure are different, where the  $\text{Yb}\cdots\text{Yb}$  separation ( $\text{Yb2}\cdots\text{Yb3}$ , 3.827(3) Å) between two  $\text{Yb}_2(\text{L})(\text{H}_2\text{L})$  portions is slightly longer than that (3.582(4)–3.602(4) Å for  $\text{Yb1}\cdots\text{Yb2}$  or  $\text{Yb3}\cdots\text{Yb4}$ ) within each portion. The solvate DMF molecule of **2**:DMF is not bound to the framework, and it exhibits no observed interactions with the host structure. As to the bulk purity of the three polycrystalline samples of complexes **1–3**, it is convincingly established by PXRD measurements. As shown in Fig. 3S, for each of the three samples, the peak positions of the measured pattern closely match those of the simulated **2**:DMF, confirming that they are really isostructural and a single phase is formed for each complex. Moreover, TGA analysis (Fig. 4S) of the three polycrystalline samples **1–3** shows the similar weight loss patterns, where a gradual weight loss (about 5%) occurred in the range of 80–140 °C, probably indicative of the loss of two coordinated EtOH molecules, and the frameworks decomposed at *ca.* 250 °C with an observed abrupt weight loss.

X-ray single-crystal structural analysis indicates that **5**:DMF:2MeOH:9H<sub>2</sub>O is typically *pseudo*-polymorphic with **2**:DMF. As shown in Fig. 2, the similar homoleptic linear tetranuclear host structure is observed from **5**:DMF:2MeOH:9H<sub>2</sub>O, while two DMF molecules are coordinated to the two corresponding outer  $\text{Yb}^{3+}$  ions in replacement with two EtOH molecules in **2**:DMF, and all the other solvates, one DMF, two MeOH and nine H<sub>2</sub>O, also have not observed interactions with the host structure. Moreover, PXRD analysis (Fig. 5S) on another series of complexes **4–6** shows that they are also iso-structural, where the measured patterns from complexes **4–6** are well consistent with the simulated pattern of

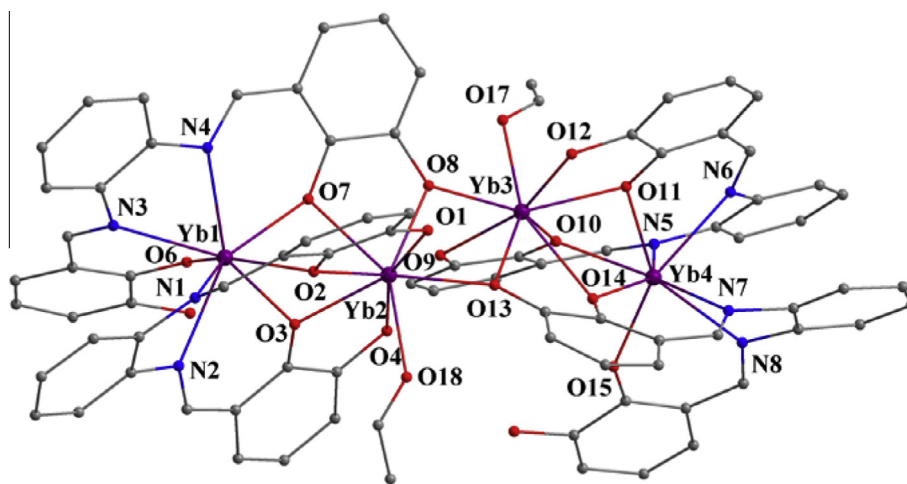


**Fig. 1.** Perspective drawing of the homoleptic linear tetranuclear framework of complex **2**:DMF, H atoms and solvate DMF are omitted for clarity.

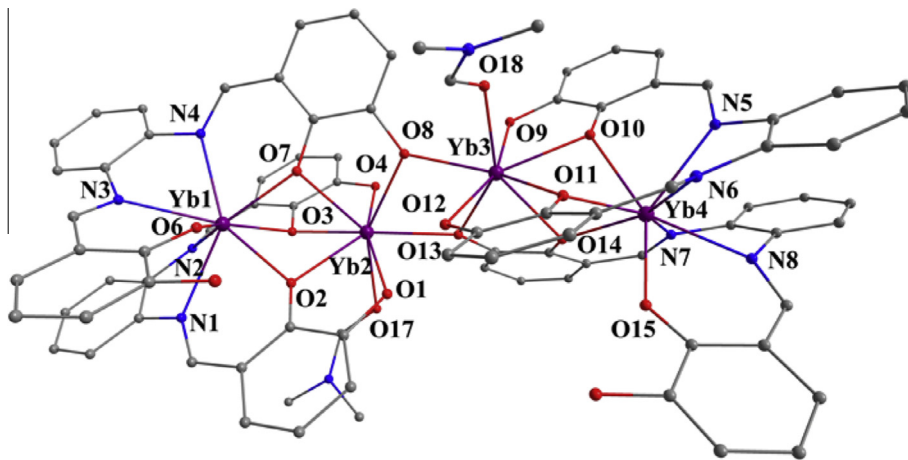


Fig. 2. Perspective drawing of the homoleptic linear tetranuclear framework of complex **5**-DMF-2MeOH-9H<sub>2</sub>O, H atoms and solvates DMF, MeOH and H<sub>2</sub>O are omitted for clarity.

**5**-DMF-2MeOH-9H<sub>2</sub>O. Similarly, TGA analysis (Fig. 6S) of three polycrystalline samples **4–6** shows the gradual weight loss (about 7%) in the range of 70–170 °C indicative of the loss of two coordinated DMF molecules and the abrupt weight loss at ca. 255 °C from decomposed frameworks. It is of interest to explore the self-assembly mechanism of the two series of homoleptic linear tetranuclear [Ln<sub>4</sub>((OH)<sub>2</sub>-Salophen)<sub>4</sub>]-arrayed complexes, where the same raw materials and reaction procedure except solvent systems are adopted. Through the use of mixed solvents EtOH–MeCN or DMF–MeCN, due to the stronger oxophilic character of Ln<sup>3+</sup> ions, the O atom of EtOH or DMF preferentially links with the hard Lewis acidic Ln<sup>3+</sup> ions, leading to the formation of two solvent-induced *pseudo*-polymorphic products. On the other hand, the use of relatively weak organic base Et<sub>3</sub>N in the two self-assembly systems endows the possibility of multiple coordination modes ((L)<sup>4-</sup>, (HL)<sup>3-</sup>, (H<sub>2</sub>L)<sup>2-</sup> or (H<sub>3</sub>L)<sup>-</sup>) shown in Scheme 1S) from the (OH)<sub>2</sub>-Salophen ligand **H<sub>4</sub>L**. The charge-balance requirement results in the co-existence of mixed (L)<sup>4-</sup>- and (H<sub>2</sub>L)<sup>2-</sup> coordination modes (in Scheme 2S) of four (OH)<sub>2</sub>-Salophen ligands while independence of different counter-anions. It is worth noting the homoleptic linear tetranuclear [Yb<sub>4</sub>((OH)<sub>2</sub>-Salophen)<sub>4</sub>] host structure in both **2**-DMF and **5**-DMF-2MeOH-9H<sub>2</sub>O is distinctively different from binuclear triple-decker Ln<sub>2</sub>(Salen)<sub>3</sub> [22] or trinuclear triple-decker Ln<sub>3</sub>(Salen)<sub>3</sub> complexes [23] from the typical quadridentate Salen-type Schiff-base ligands, and also incomparable to trinuclear triple-decker Ln<sub>3</sub>(Salen)<sub>3</sub> [24], cyclic tetranuclear Ln<sub>4</sub>(Salen)<sub>4</sub> [25] or Ln<sub>4</sub>(Salen)<sub>2</sub> [26] and pentanuclear tetra-decker Ln<sub>5</sub>(Salen)<sub>4</sub> [27] frameworks from the hexadentate Salen-type Schiff-base ligands with two –OMe groups, where the charge balance inevitably depends on the counter-anions.

#### Photophysical properties of complexes **2–3** and **5–6**

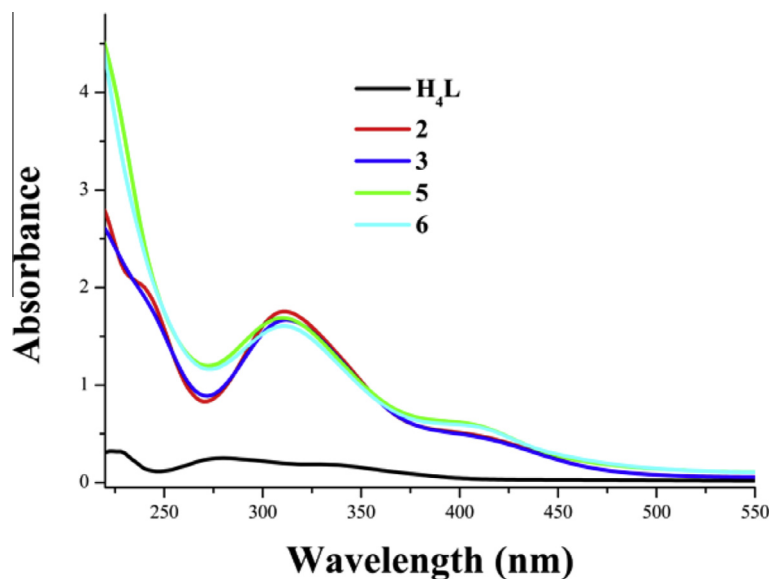
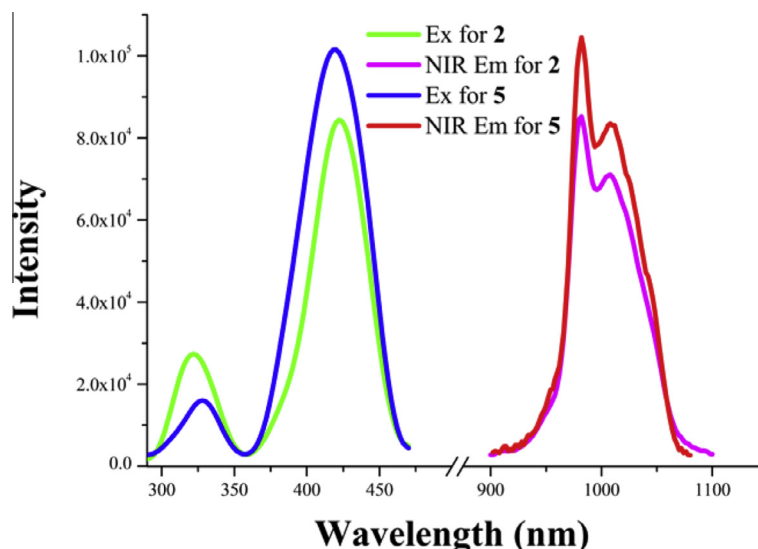
The photophysical properties of the ligand **H<sub>4</sub>L** and two series of complexes **2–3** and **5–6** have been examined in dilute DMSO at room temperature or 77 K, and summarized in Table 2, and Figs. 3–5. As shown in Fig. 3, the similar ligand-centered solution absorptions, 238–239, 312–314 and 410–412 nm for complexes **2–3** and 230–232, 310–312 and 409–410 nm for complexes **5–6** in the UV–visible region are shown, respectively. Both are distinctively red-shifted up coordination of Ln<sup>3+</sup> ions compared to that (228, 280 and 336 nm) of the free (OH)<sub>2</sub>-Salophen ligand **H<sub>4</sub>L**. It is worth noting that the almost identical maximum positions and molar absorption coefficients with four orders of magnitude larger than that of the ligand **H<sub>4</sub>L** in all the four lowest energy bands

(409–412 nm) are observed for the two series of four complexes, which should be resulted from the involvement of four equivalent chromophores with similar arrangement. For both **2** and **5**, the almost similar residual weak visible emissions ( $\lambda_{em} = ca. 483$  nm,  $\tau < 1$  ns and  $\Phi_{em} < 10^{-5}$ ) in dilute absolute DMSO solution at room temperature are observed, while photo-excitation of the chromophore in the range 270–470 nm ( $\lambda_{ex} = ca. 420$  nm), as shown in Fig. 4, gives rise to the similar strong characteristic ligand-field emission of the Yb<sup>3+</sup> ion ( $\lambda_{em} = 982$  nm,  $^2F_{5/2} \rightarrow ^2F_{7/2}$ ), respectively. As to the free ligand **H<sub>4</sub>L** and two [Gd<sub>4</sub>((OH)<sub>2</sub>-Salophen)<sub>4</sub>] complexes **3** and **6**, they just display the typical luminescence emissions (Fig. 5) of the Schiff-base ligand in the visible range. It is noticeable that the excitation spectra of [Yb<sub>4</sub>((OH)<sub>2</sub>-Salophen)<sub>4</sub>]-containing complexes **2** and **5** monitored at the “hypersensitive” NIR emission peak are similar to those of [Gd<sub>4</sub>((OH)<sub>2</sub>-Salophen)<sub>4</sub>] complexes **3** and **6**, demonstrating that both of the NIR luminescent emissions for **2** and **5** originate from Yb<sup>3+</sup> ion upon sensitization through the antenna effect [28]. Especially based on the check of the luminescence for the respective [Gd<sub>4</sub>((OH)<sub>2</sub>-Salophen)<sub>4</sub>]-based complex **3** or **6** at 77 K, the strengthened while also typical fluorescence ( $\lambda_{em} = 470$ –473 nm,  $\tau = 6.21$ –6.31 ns and  $\lambda_{em} = 548$ –551 nm,  $\tau = 12.56$ –12.64 ns, as shown in Table 2), shows that the sensitization of the NIR luminescence for both **2** and **5** should arise from the similar <sup>1</sup>LC (18,180 cm<sup>-1</sup>) excited state of the (OH)<sub>2</sub>-Salophen ligand **H<sub>4</sub>L** especially at low temperature [29].

In consideration of the similar [Yb<sub>4</sub>((OH)<sub>2</sub>-Salophen)<sub>4</sub>] host structure while two different coordinated solvents (EtOH or DMF) embracing two central Yb<sup>3+</sup> ions for the two *pseudo*-polymorphic complexes **2** and **5**, we were interested in the NIR luminescence difference caused by OH- and/or CH-containing oscillators (solvents) vibrations. For a meaningful comparison, the relative emission intensity of **5** is about 1.3 times to that of **2** at 982 nm when their concentrations are adjusted to give the same absorbance value at 410 nm. Further through time-resolved luminescent experiments under the same condition, their two luminescent decay curves (Fig. 7S) can be fitted mono-exponentially with time constants of microseconds (11.72  $\mu$ s for **2** or 18.39  $\mu$ s for **5**), and their NIR intrinsic quantum yields  $\Phi_{Yb}$  (0.59% for **2** or 0.92% for **5**) of the Yb<sup>3+</sup> emissions may be estimated by  $\Phi_{Yb} = \tau_{obs}/\tau_0$ , where  $\tau_{obs}$  is the observed emission lifetime and  $\tau_0$  is the “neutral lifetime” viz 2.0 ms for Yb<sup>3+</sup> ion [30]. Both demonstrate that the NIR luminescent property of the Yb<sup>3+</sup> ion in complexes **2** and **5** is sensitive to solvents-based oscillator vibrations within the inner coordination spheres of Yb<sup>3+</sup> ions. As a matter of fact, the NIR emission of Ln<sup>3+</sup> ions critically depends

**Table 2**The photophysical properties of the ligand **H<sub>4</sub>L** and complexes **2–3** and **5–6** at  $2 \times 10^{-5}$  M in absolute DMSO solution at room temperature or 77 K.

Compound	Absorption $\lambda_{ab}$ (nm) [ $\log(\epsilon/\text{dm}^3 \text{ mol}^{-1} \text{ cm}^{-1})$ ]	Excitation $\lambda_{ex}$ (nm)	Emission $\lambda_{em}$ (nm) ( $\tau$ , $\Phi \times 10^3$ )
H <sub>4</sub> L	228(0.32), 280(0.25), 336(0.13)	321	491(m, 2.45 ns, 38.6)
2	238(2.00), 312(1.75), 410(0.49)	322(sh), 421	482(w, <1 ns, <10 <sup>-2</sup> ), 982(split, 11.72 $\mu$ s)
3	239(1.97), 314(1.67), 412(0.48)	324(sh), 419	482(m), 504(m, 1.79 ns, 14.2) 470(s, 6.21 ns, 77 K), 548(12.56 ns)
5	232(3.30), 310(1.69), 409(0.55)	328(sh), 420	484(w, <1 ns, <10 <sup>-2</sup> ), 982(split, 18.39 $\mu$ s)
6	230(3.19), 312(1.61), 410(0.53)	323(sh), 417	484(m), 501(m, 1.68 ns, 13.1) 473(s, 6.31 ns, 77 K), 551(s, 12.64 ns, 77 K)

**Fig. 3.** UV-visible absorption spectra of the ligand **H<sub>4</sub>L** and two series of complexes **2–3** and **5–6** in DMSO solution at  $2 \times 10^{-5}$  M at room temperature.**Fig. 4.** NIR emission and excitation spectra of complexes **2** and **5** in DMSO solution at  $2 \times 10^{-5}$  M at room temperature.

on the coupling of the excited state of  $\text{Ln}^{3+}$  ion with vibrations of nearby oscillators [31]. Moreover, the relatively lower frequency ( $\nu_{\text{sym}} = 2900\text{--}3100 \text{ cm}^{-1}$ ) of  $-\text{CH}$  vibration than that ( $\nu_{\text{sym}} = 3400\text{--}3700 \text{ cm}^{-1}$ ) of  $-\text{OH}$  vibration has a negative influence on the effectiveness of luminescence [32]. Therefore, although the equivalent energy gap ( $\Delta E = 7780 \text{ cm}^{-1}$ ) between the excited states of the same organic chromophore and  $\text{Yb}^{3+}$

ion is observed for the two *pseudo*-polymorphic complexes **2** and **5**, the better NIR luminescent property of **5** than that of **2** with one nearby  $-\text{OH}$  ( $\nu_1$ ) and five relatively distant  $-\text{CH}$  (two  $\nu_2$  and three  $\nu_3$ ) oscillators from the two coordinated EtOH molecules, should be resulted from the scarcity of nearby oscillators for **5** despite relatively distant  $-\text{CH}$  (one  $\nu_2$  and six  $\nu_3$ ) oscillators from two coordinated DMF molecules.

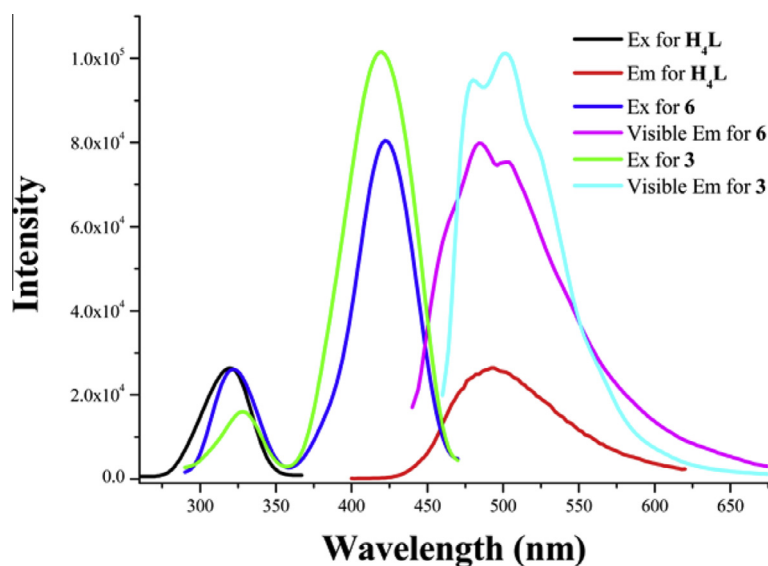


Fig. 5. Visible emission and excitation spectra of the ligand  $\text{H}_4\text{L}$  and complexes **3** and **6** in DMSO solution at  $2 \times 10^{-5}$  M at room temperature.

## Conclusions

In conclusion, two series of anion-independent while *pseudo*-polymorphic homoleptic linear tetranuclear complexes  $[\text{Ln}_4(\text{H}_2\text{L})_2(\text{L})_2(\text{EtOH})_2]$  ( $\text{Ln} = \text{La}$ , **1**;  $\text{Ln} = \text{Yb}$ , **2** or  $\text{Ln} = \text{Gd}$ , **3**) and  $[\text{Ln}_4(\text{H}_2\text{L})_2(\text{L})_2(\text{DMF})_2]$  ( $\text{Ln} = \text{La}$ , **4**;  $\text{Ln} = \text{Yb}$ , **5** or  $\text{Ln} = \text{Gd}$ , **6**) are obtained from the self-assembly of the dihydroxyl-modified  $(\text{OH})_2$ -Salophen ligand  $\text{H}_4\text{L}$  with  $\text{LnCl}_3 \cdot 6\text{H}_2\text{O}$  or  $\text{Ln}(\text{NO}_3)_3 \cdot 6\text{H}_2\text{O}$  in mixed solvents MeCN–EtOH and MeCN–DMF, respectively. The result of their photophysical properties shows that the  $(\text{OH})_2$ -Salophen ligand may work as antennae for effective sensitization of the characteristic NIR luminescence of  $\text{Yb}^{3+}$  ions for both  $[\text{Yb}_4(\text{H}_2\text{L})_2(\text{L})_2(\text{EtOH})_2]$  (**2**) and  $[\text{Yb}_4(\text{H}_2\text{L})_2(\text{L})_2(\text{DMF})_2]$  (**5**), while the scarcity of nearby oscillators, together with distant relatively lower-frequency –CH vibrations from two coordinated DMF molecules in **5** endows the relatively higher NIR quantum yield (0.92%). The specific design of polynuclear  $\text{Yb}^{3+}$  complexes from the flexible  $(\text{OH})_2$ -Salen ligands by further deep deprotonations in facilitating the NIR sensitization is now under way.

## Acknowledgements

This work is funded by the National Natural Science Foundation (21373160, 91222201, 21173165), the Program for New Century Excellent Talents in University from the Ministry of Education of China (NCET-10-0936), the Doctoral Program (20116101110003) of Higher Education, the Education Committee Foundation (11JK0588), the Science, Technology and Innovation Project (2012KTCQ01-37) of Shaanxi Province and Hong Kong Research Grants Council (HKBU 202407 and FRG/06-07/II-16) in P.R. of China, the Robert A. Welch Foundation (Grant F-816), the Texas Higher Education Coordinating Board (ARP 003658-0010-2006), and the Petroleum Research Fund, administered by the American Chemical Society (47014-AC5).

## Appendix A. Supplementary data

Supplementary data associated with this article can be found, in the online version, at <http://dx.doi.org/10.1016/j.saa.2015.01.082>.

The coordination modes for the common  $(\text{OH})_2$ -Salen Schiff-base ligand ( $\text{H}_4\text{L}^0$ ) or the  $(\text{OH})_2$ -Salophen ligand ( $\text{H}_4\text{L}$ ) in Schemes 1S and 2S, respectively; selected bond lengths and bond angles for complexes **2**-DMF and **5**-DMF·2MeOH·9H<sub>2</sub>O in Table 1S, <sup>1</sup>H

NMR spectra data of  $\text{H}_4\text{L}$  in  $\text{CDCl}_3$  and two *anti*-ferromagnetic  $[\text{La}_4((\text{OH})_2\text{-Salophen})_4]$ -arrayed complexes **1** and **4** in DMSO- $\delta_6$  in Fig. 1S, ESI-MS data of polycrystalline samples of complexes **1–6** in dilute DMSO in Fig. 2S, PXRD and TGA results for complexes **1–3** and **4–6** in Figs. 3S–6S and luminescent decay profiles for complexes **2** and **5** in Fig. 7S, respectively. The crystallographic data for complexes **2**-DMF and **5**-DMF·2MeOH·9H<sub>2</sub>O have been deposited at the Cambridge Crystallographic Data Center, CCDC-1000322 (for **2**-DMF) and CCDC-1000323 (for **5**-DMF·2MeOH·9H<sub>2</sub>O). The data can be obtained free of charge via <http://www.ccdc.cam.ac.uk/conts/retrieving.html> or from the Cambridge CB21E2, UK.

## References

- [1] M.A. Katkova, M.N. Bochkarev, New trends in design of electroluminescent rare earth metallo-complexes for OLEDs, Dalton Trans. 39 (2010) 6599–6612.
- [2] S.V. Eliseeva, J.-C.G. Bünzli, Lanthanide luminescence for functional materials and bio-sciences, Chem. Soc. Rev. 39 (2010) 189–227.
- [3] M.C. Heffern, L.M. Matosziuk, T.G. Meade, Lanthanide probes for bio-responsive imaging, Chem. Rev. 114 (2014) 4496–4539.
- [4] S. Comby, J.-C.G. Bünzli, in: K.A. Gschneidner Jr., J.-C.G. Bünzli, V.K. Pecharsky (Eds.), Handbook on the Physics and Chemistry of Rare Earths, Elsevier Science B.V., Amsterdam, 2007, vol. 37 (Chapter 235).
- [5] X.P. Yang, R.A. Jones, Anion dependent self-assembly of “tetra-decker” and “triple-decker” luminescent Tb(III) Salen complexes, J. Am. Chem. Soc. 127 (2005) 7686–7687.
- [6] X.P. Yang, R.A. Jones, M.M. Oye, M. Wiester, R.J. Lai, Influence of metal-ligand ratio on benzimidazole based luminescent lanthanide complexes: 3-D network structures and chloride anion binding, New J. Chem. 35 (2011) 310–318.
- [7] J.-C.G. Bünzli, C. Piguet, Taking advantage of luminescent lanthanide ions, Chem. Soc. Rev. 34 (2005) 1048–1077.
- [8] J.-C.G. Bünzli, S. Comby, A.S. Chauvin, C.D.B. Vandevyver, New opportunities for lanthanide luminescence, J. Rare Earths 25 (2007) 257–274.
- [9] L. Winkless, R.H.C. Tan, Y. Zheng, M. Motevalli, P.B. Wyatt, W.P. Gillin, Quenching of Er(III) luminescence by C-H vibrations: implications for the use of erbium complexes in telecommunications, Appl. Phys. Lett. 89 (2006) 111115-1-3.
- [10] K. Biradha, C.Y. Su, J.J. Vittal, Recent developments in crystal engineering, Cryst. Growth Des. 11 (2011) 875–886.
- [11] X.J. Zhu, W.-K. Wong, W.-Y. Wong, X.P. Yang, Design and synthesis of near-infrared emissive lanthanide complexes based on macrocyclic ligands, Eur. J. Inorg. Chem. (2011) 4651–4674.
- [12] X.Q. Lü, W.X. Feng, Y.N. Hui, T. Wei, J.R. Song, S.S. Zhao, W.-Y. Wong, W.-K. Wong, R.A. Jones, Near-Infrared luminescent, neutral, cyclic  $\text{Zn}_2\text{Ln}_2$  ( $\text{Ln} = \text{Nd}$ ,  $\text{Yb}$ , and  $\text{Er}$ ) complexes from asymmetric salen-type schiff base ligands, Eur. J. Inorg. Chem. (2010) 2714–2722.
- [13] S. Liao, X.P. Yang, R.A. Jones, Self-assembly of luminescent hexanuclear lanthanide salen complexes, Cryst. Growth Des. 2 (2012) 970–974.
- [14] M.M. Belmonte, E.C. Escudero-Adán, E. Martín, A.W. Kleij, Isolation and characterization of unusual multinuclear Schiff base complexes: rearrangements reactions and octanuclear cluster formation, Dalton Trans. 41 (2012) 5193–5200.

- [15] L. Salmon, P. Thuery, M. Ephritikhine, Crystal structure of the first octanuclear uranium(IV) complex with compartmental schiff base ligands, *Polyhedron* 23 (2004) 623–627.
- [16] K. Bhattacharya, M. Maity, S.M.T. Abtab, M.C. Majee, M. Chaudhury, Homo- and heterometal complexes of oxido-metal ions with a triangular [V(V)O-MO-V(V)O] [M = V(IV) and Re(V)] core: reporting mixed-oxidation oxido-vanadium(V/IV/V) compounds with valence trapped structures, *Inorg. Chem.* 52 (2013) 9597–9605.
- [17] L. Salmon, P. Thuéry, M. Ephritikhine, Strictly heterodinuclear compounds containing U<sup>4+</sup> and Cu<sup>2+</sup> or Ni<sup>2+</sup> ions, *Polyhedron* 26 (2007) 645–652.
- [18] L. Salmon, P. Thuéry, M. Ephritikhine, Synthesis and crystal structure of uranium(IV) complexes with compartmental schiff bases: from mononuclear species to tri- and tetranuclear clusters, *Dalton Trans.* (2004) 1635–1643.
- [19] R.M. Haak, A. Decortes, E.C. Escudero-Adan, M.M. Belmonte, E. Martin, J. Benet-Buchholz, A.W. Kleij, Shape-persistent octanuclear zinc Salen clusters: synthesis, characterization, and catalysis, *Inorg. Chem.* 50 (2011) 7934–7936.
- [20] G.M. Sheldrick, SHELXL-97: Program for Crystal Structure Refinement, Göttingen, Germany, 1997.
- [21] G.M. Sheldrick, SADABS, University of Göttingen, 1996.
- [22] P.F. Yang, S. Chen, J.W. Zhang, G.M. Li, Novel quadridentate salen type triple-decker sandwich ytterbium complexes with near infrared luminescence, *CrystEngComm* 13 (2011) 36–39.
- [23] F. Yang, P.F. Yan, Q. Li, P. Chen, G.M. Li, Salen-type triple-decker trinuclear Dy<sub>3</sub> complexes showing slow magnetic relaxation behavior, *Eur. J. Inorg. Chem.* (2012) 4287–4293.
- [24] X.P. Yang, R.A. Jones, M.M. Oye, A.L. Holmes, W.-K. Wong, Near infrared luminescence and supramolecular structure of a helical triple-decker Yb(III) Schiff base cluster, *Cryst. Growth Des.* 6 (2006) 2122–2125.
- [25] W.X. Feng, Y. Zhang, X.Q. Lü, Y.N. Hui, G.X. Shi, D. Zou, J.R. Song, D.D. Fan, W.-K. Wong, R.A. Jones, Near-infrared (NIR) luminescent homoleptic lanthanide salen complexes Ln<sub>4</sub>(Salen)<sub>4</sub> (Ln = Nd, Yb or Er), *CrystEngComm* 14 (2012) 3456–3463.
- [26] W.X. Feng, Y. Zhang, Z. Zhang, X.Q. Lü, H. Liu, G.X. Shi, D. Zou, J.R. Song, D.D. Fan, W.-K. Wong, R.A. Jones, Anion-induced self-assembly of luminescent and magnetic homoleptic cyclic tetranuclear Ln<sub>4</sub>(salen)<sub>4</sub> and Ln<sub>4</sub>(salen)<sub>2</sub> complexes (Ln = Nd, Yb, Er, or Gd), *Inorg. Chem.* 51 (2012) 11377–11386.
- [27] X.P. Yang, R.A. Jones, W.-K. Wong, Pentanuclear tetra-decker luminescent lanthanide Schiff base complexes, *Dalton Trans.* (2008) 1676–1678.
- [28] J.-C.G. Bünzli, Lanthanide luminescence for biomedical analyses and imaging, *Chem. Rev.* 110 (2010) 2729–2755.
- [29] W.Y. Bi, T. Wei, X.Q. Lü, Y.N. Hui, J.R. Song, S.S. Zhao, W.-K. Wong, R.A. Jones, Hetero-trinuclear near-infrared (NIR) luminescent Zn<sub>2</sub>Ln complexes from Salen-type Schiff-base ligands, *New J. Chem.* 33 (2009) 2326–2334.
- [30] M.J. Weber, Radiative and multiphonon relaxation of rare-earth ions in Y<sub>2</sub>O<sub>3</sub>, *Phys. Rev.* 171 (1968) 283–291.
- [31] G.A. Hebbink, D.N. Reinhoudt, F.C.J.M. van Veggel, Increased luminescent lifetimes of Ln<sup>3+</sup> complexes emitting in the near-infrared as a result of deuteration, *Eur. J. Org. Chem.* (2001) 4101–4106.
- [32] C. Doffek, N. Alzakhem, C. Bischof, J. Wahsner, T. Güden-Silber, J. Lügger, C. Platas-Iglesias, M. Seitz, Understanding the quenching effects of aromatic C-H and C-D oscillators in near-IR lanthanoid luminescence, *J. Am. Chem. Soc.* 134 (2012) 16413–16423.